AGU PUBLICATIONS

Geophysical Research Letters

RESEARCH LETTER
10.1002/2016GL069544

Key Points:
- Atlantic SST anomalies contribute to generation of Pacific decadal variability
- Equatorial and South Atlantic SST trends reorganize global Walker Circulation
- Phase of Interdecadal Pacific Oscillation influenced by SST anomalies in other ocean basins

Supporting Information:
- Supporting Information S1

Correspondence to:
Y. Chikamoto,
chika44@hawaii.edu

Citation:
Chikamoto, Y., T. Mochizuki, A. Timmermann, M. Kimoto, and M. Watanabe (2016), Potential tropical Atlantic impacts on Pacific decadal climate trends, *Geophys. Res. Lett.*, *43*, doi:10.1002/2016GL069544.

Received 16 DEC 2015
Accepted 14 JUN 2016
Accepted article online 20 JUN 2016

Potential tropical Atlantic impacts on Pacific decadal climate trends

Y. Chikamoto[1], T. Mochizuki[2], A. Timmermann[1], M. Kimoto[3], and M. Watanabe[3]

[1]International Pacific Research Center, University of Hawaii at Manoa, Honolulu, Hawaii, USA, [2]Japan Agency for Marine-Earth Science and Technology, Yokohama, Japan, [3]Atmosphere and Ocean Research Institute, University of Tokyo, Kashiwa, Japan

Abstract The tropical Pacific cooling from the early 1990s to 2013 has contributed to the slowdown of globally averaged sea surface temperatures (SSTs). The origin of this regional cooling trend still remains elusive. Here we demonstrate that the remote impact of Atlantic SST anomalies, as well as local atmosphere-ocean interactions, contributed to the eastern Pacific cooling during this period. By assimilating observed three-dimensional Atlantic temperature and salinity anomalies into a coupled general circulation model, we are able to qualitatively reproduce the observed Pacific decadal trends of SST and sea level pressure (SLP), albeit with reduced amplitude. Although a major part of the Pacific SLP trend can be explained by equatorial Pacific SST forcing only, the origin of this low-frequency variability can be traced back further to the remote impacts of equatorial Atlantic and South Atlantic SST trends. Atlantic SST impacts on the atmospheric circulation can also be detected for the Northeastern Pacific, thus providing a linkage between Atlantic climate and Western North American drought conditions.

1. Introduction

The period from ~2000 to 2013 C.E. was characterized by a slowdown of global mean sea surface temperature (SST) relative to the period from 1970 to 2000. This slowdown can be attributed to a prominent cooling of the eastern equatorial Pacific [*Kosaka and Xie*, 2013; *Watanabe et al.*, 2013; *England et al.*, 2014; *McGregor et al.*, 2014; *Meehl and Teng*, 2014]. On average, externally forced twentieth century coupled general circulation model (CGCM) simulations do not reproduce a reduced warming trend for this particular period [*Easterling and Wehner*, 2009; *Kosaka and Xie*, 2013; *Watanabe et al.*, 2013]. A number of recent studies [e.g., *Meehl et al.*, 2011; *Kosaka and Xie*, 2013; *Trenberth and Fasullo*, 2013; *England et al.*, 2014] investigated the underlying physical mechanisms and found that the Pacific cooling was accompanied by a record-breaking equatorial Pacific trade wind intensification and its corresponding acceleration of sea level rise in the western tropical Pacific [*Timmermann et al.*, 2010; *Merrifield and Maltrud*, 2011; *McGregor et al.*, 2014; *Han et al.*, 2014]. Furthermore, the eastern Pacific cooling trend affected the global atmospheric circulation, which in turn caused winter cooling in northwestern North America and enhanced drought conditions in the southwestern United States [*Kosaka and Xie*, 2013; *McGregor et al.*, 2014; *Meehl and Teng*, 2014; *Delworth et al.*, 2015] due to the establishment of a pronounced anticyclonic circulation over the eastern subtropical Pacific (Figures S1a–S1c and S2a–S2c in the supporting information).

The origin of the recent decadal-scale Pacific cooling trend, which projects onto the negative phase of the Interdecadal Pacific Oscillation (IPO), can be partly traced back to the Atlantic warming trend [*Kucharski et al.*, 2011; *Chikamoto et al.*, 2012; *McGregor et al.*, 2014; *Chikamoto et al.*, 2015; *Li et al.*, 2015b]. In the early 1990s, a negative trend of the North Atlantic Oscillation contributed to a rapid SST warming in the North Atlantic as well as the tropical Atlantic [*Robson et al.*, 2012; *Yeager et al.*, 2012]. This temperature anomaly enhanced the thermal contrast between Atlantic and Pacific, which resulted in large-scale shifts of the global sea level pressure (SLP) distribution and its corresponding reorganization of the global Walker Circulation [*Chikamoto et al.*, 2012; *McGregor et al.*, 2014; *Chikamoto et al.*, 2015; *Kucharski et al.*, 2015]. According to this scenario, a subsequent intensification of the surface trade winds in the equatorial Pacific then caused a gradual cooling in the eastern tropical Pacific as well as the acceleration of sea level rise in the western tropical Pacific [*England et al.*, 2014; *McGregor et al.*, 2014]. Positive air-sea feedbacks in the Pacific then further intensified the local responses. Even though there is growing scientific evidence supporting an Atlantic role in decadal Pacific

climate variability, it still remains unclear, which part of Atlantic SST variability contributed to the Pacific decadal trends in temperature, SLP, and winds.

Using the partial ocean data assimilation approach as described in section 2, we identify the relative roles of equatorial, North, and South Atlantic forcing on Pacific decadal trends.

2. Partial Assimilation Experiments

Using the coupled atmosphere-ocean general circulation model, MIROC3.2m [*Nozawa et al.*, 2007], we conducted a series of historical forcing and assimilation runs. The atmospheric component has T42 spectral truncation with 20 vertical σ levels. The ocean component uses a horizontal resolution of 1.4° in longitude and 0.56–1.4° in latitude with 44 vertical levels. These components exchange heat, momentum, and water fluxes with each other as well as with the land and sea ice modules. In the ensemble of historical simulations (hereafter HIST), we prescribe for the period of 1850–2010 C.E. natural and anthropogenic radiative forcings (observed and following A1B-type emission scenario) [*Nakicenovic et al.*, 2000]. A total of 10 ensemble members is used starting from different initial conditions obtained from the preindustrial control simulation. For the 10-member global ocean observation assimilation runs (GLOB), the model climatology defined by the 1961–1990 period from the HIST run is added onto the observed three-dimensional oceanic temperature and salinity anomalies from surface to 700 m depth during the period of 1945–2010 [*Ishii and Kimoto*, 2009]. The assimilation runs also use the same external radiative forcings as the HIST run (solar, aerosols, land-use change, and greenhouse gases). The anomalies outside the sea ice regions are assimilated into the coupled climate model using the incremental analysis update scheme [*Bloom et al.*, 1996; *Huang et al.*, 2002]. Details of the model experiments can be found in *Mochizuki et al.* [2010] and *Chikamoto et al.* [2015].

To evaluate the impact of equatorial Pacific SST variability on the Atlantic or the impact of Atlantic variability on the Pacific, we partially assimilate the observed ocean temperature and salinity anomalies in either the equatorial Pacific (10°S–10°N; eqPAC), the entire Atlantic (50°S–60°N; ATL), the North Atlantic (10°N–60°N; NATL), the equatorial Atlantic (10°S–10°N; eqATL), and the South Atlantic oceans (40°S–10°S; SATL). These partial assimilation experiments consist of 10-member ensembles each and cover the period from 1945 to 2010. The partial assimilation experiments capture not only the low-frequency atmospheric response to the SST variability in the assimilated area but also allow for responses that are based on remote air-sea interactions. In addition, our subsurface temperature and salinity assimilation contributes to initialize the low-frequency ocean signals by reducing high-frequency noises originated from atmospheric disturbances. Similar experiments with partial assimilation or nudging have been conducted by others [*Zhang and Delworth*, 2007; *Kosaka and Xie*, 2013; *McGregor et al.*, 2014; *Chikamoto et al.*, 2015; *Kucharski et al.*, 2015; *Li et al.*, 2015b].

Anomalies are defined as deviations from the climatological mean for 1980–1999 in each experiment and the observations. For model validation, surface air temperature (SAT), SLP, and SST observational estimates are used from HadCRUT version 4.4.0.0 [*Morice et al.*, 2012], HadSLP2r [*Allan and Ansell*, 2006], ERA-Interim [*Dee et al.*, 2011], and ERSST version 4 [*Huang et al.*, 2015].

3. Impacts of Atlantic Ocean on the Pacific Climate Change

Our global ocean assimilation experiment GLOB reproduces the observed global SAT anomalies very well (Figure 1a). In particular, the GLOB simulation captures the Global Warming Hiatus (GWH), relative to the externally forced simulation HIST (Figure 1a, blue line and shading), in good agreement with the observations (Figure 1, dotted and dashed lines). This indicates that land surface temperature changes, such as a pronounced seasonal cooling over Siberia [*Li et al.*, 2015a] as well as forcings from unaccounted volcanic aerosols and stratospheric water vapor changes, only played a secondary role in the recent slowdown of surface temperatures. To highlight the decadal climate trends, we calculate the 9 year running trends of SAT and SLP anomalies (Figure 1b). The recent GWH is characterized by the deviation between simulated 9 year running trends of the SAT in GLOB and HIST (bars in Figure 1b). The two peaks of 9 year cooling trends for the 1992–2000 and 2001–2009 periods (plotted as 1992 and 2001 in Figure 1b) mark particularly strong anomalies during the GWH period (Figures S1 and S2). Temporal variations of unforced 9 year global mean SAT trends are tightly linked with the natural decadal SAT trends in the eastern tropical Pacific (red line in Figure 1b; correlation coefficient $R = 0.65$). Furthermore, the ensemble experiment using three-dimensional ocean data assimilation only in the equatorial Pacific (eqPAC) highlights the importance of Pacific decadal variability in

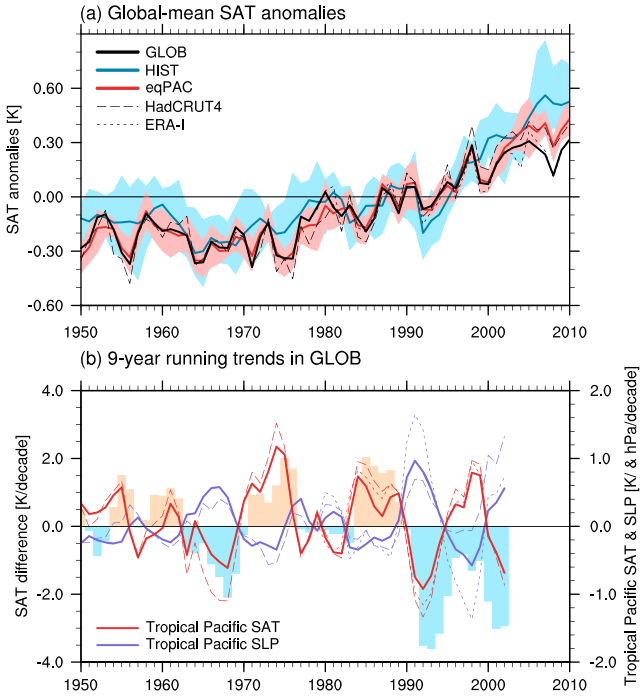

Figure 1. Time series of (a) global mean SAT anomalies in the GLOB (black), HIST (blue), eqPAC runs (red), HadCRUT4 (dashed), and ERA-I (dotted). Line and shading represent the ensemble mean and the maximum-minimum ensemble range, respectively. Time series of (b) 9 year running trends of the global mean SAT difference between GLOB and HIST (shading), the eastern tropical Pacific SAT (10°S–10°N, 170°W–120°W; red line), and the central tropical Pacific SLP (15°S–15°N, 180°–150°W; purple line). The time for each trend is calculated at the beginning year of 9 year trend. Solid, dashed, and dotted lines are the GLOB run, HadCRUT4/HadSLP2r, and ERA-I data, respectively.

determining the variability around the externally forced global mean SAT trend (Figure 1a, red line). Our results confirm previous studies that identified the tropical eastern Pacific cooling as the main culprit of the GWH [*Meehl et al.*, 2011; *Kosaka and Xie*, 2013; *Nieves et al.*, 2015]. We also find that SLP running trends in the central tropical Pacific are correlated with the Pacific decadal SAT trends, with the former leading the latter by 1 year (the 1 year lagged correlation coefficient between blue and red solid lines in Figure 1b is −0.81; see Figure S3). This supports the scenario that SLP-induced surface wind forcing was partly responsible for the eastern tropical Pacific SST changes and their subsequent effect on global mean surface temperature.

Here we further explore the causes for the recent equatorial trade wind acceleration and whether surface temperature trends in other ocean basins played a role in its genesis. In order to detect the coherent SLP variability between the observations and our CGCM experiments with partial ocean data assimilation, we apply singular value decomposition (SVD) analysis to the 9 year running trends of Pacific SLP anomalies (50°S–70°N, 120°E–90°W) in the observations and the model simulations (GLOB, eqPAC, and ATL). The first SVD SLP trend mode for the observations and the GLOB run explains 81.9% in total covariance (Figure 2a). The associated SLP eigenmodes are very similar with each other (Figures 2a and 2b, contours), which are characterized by a reorganization of the global Walker Circulation with anomalously low SLP in the Indian and western Pacific regions and anomalously high values in the eastern Pacific. The respective principal component time series are highly correlated with each other ($R = 0.87$, Figure 2c) and are also closely aligned with temporal variations of the 9 year running trends of tropical Pacific SAT and SLP anomalies with local peaks around 1992 and 2001 (red and purple lines in Figure 1b; $R = -0.79$ and 0.84, respectively). We further calculate the associated correlation patterns for SST (Figures 2a and 2b, shading). The global transbasin SLP reorganization is linked to a similar large-scale shift in the transbasin contrast of SST between the Atlantic and the Pacific (Figures 2a and 2b, shading).

In contrast to the GLOB simulation, which captures well the observed evolution of transbasin SST and SLP variability, the externally forced HIST simulation (Figures 2d, 2e, S1d, and S2d) exhibits a very different behavior. The corresponding SLP SVD mode of HIST and the observations (explaining 49.6% of the covariance) shows

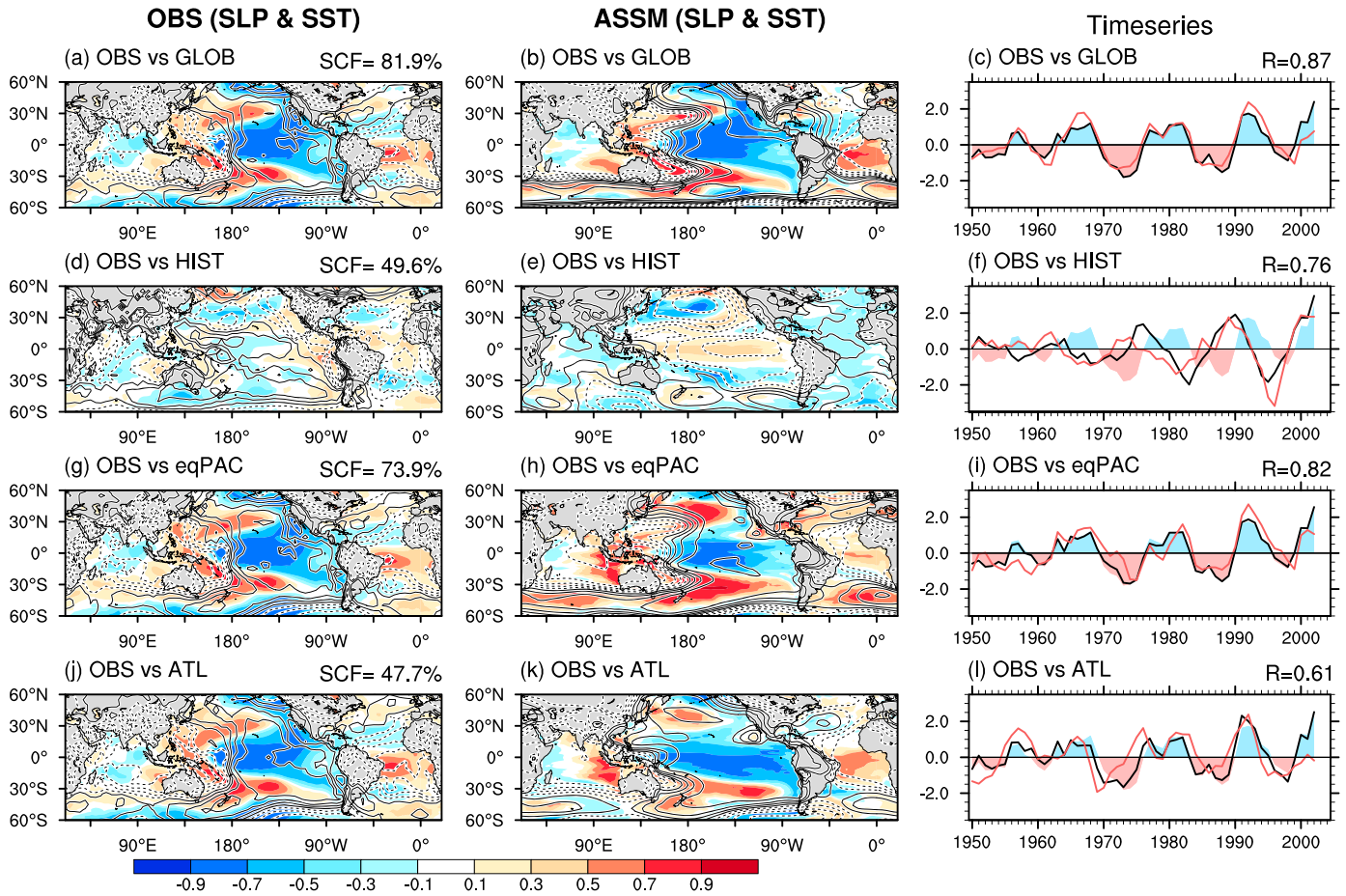

Figure 2. Correlation patterns of SST (shade) and SLP (contour) associated with the first SVD mode between the (a, d, g, and j) observed and (b, e, h, and k) the model simulated 9 year Pacific SLP running trends in (a, b) GLOB, (d, e) HIST, (g, h) eqPAC, and (j, k) ATL runs. Observed SLP and SST are obtained from HadSLP2r and ERSST data sets. The squared covariance fraction (SCF) explained by the first SVD mode and the temporal correlation coefficient (*R*) between the expansion coefficients of observations and model simulation are indicated in Figures 2a, 2d, 2g, and 2j and Figures 2c, 2f, 2i, and 2l, respectively. Negative contours are dashed and zero contours are omitted. Contour intervals are ±0.1, ±0.3, ±0.5, ±0.7, and ±0.9. (c, f, i, and l) The principal components of the first SVD mode between observation (black) and model simulations (red) in (c) GLOB, (f) HIST, (i) eqPAC, and (l) ATL runs. Shadings in Figures 2c, 2f, 2i, and 2l correspond to the black line in Figure 2c.

coherent variability with markedly different associated patterns and principal components than for GLOB (Figure 2f). In fact, the SVD principal component time series for observations and HIST are uncorrelated with those for GLOB (black line and color bars in Figure 2f; $R = 0.07$), suggesting a minor contribution from the external forcing to the Pacific SLP trends.

Consistent with previous studies, our eqPAC run demonstrates that equatorial Pacific SST forcing is the major contributor to the Pacific SLP trends, explaining 73.9% of total covariance (Figures 2g–2i). Interestingly, for this run, we also find coherent SLP and SST variability in the Atlantic region, which points to a pronounced two-basin interaction. A similar analysis for the ATL experiment (Figures 2j–2l) identifies the first SVD mode (explaining 47.7% of the covariance) as a transbasin seesaw in SLP and SST, with large similarities to the GLOB and eqPAC simulations, but with a smaller explained covariance. These similarities indicate that a considerable fraction of the low-frequency Pacific variability can in fact be reproduced simply by Atlantic SST forcing. Focusing just on the period 1992–2000, we also see that the eastern Pacific cooling trend can be partly reproduced through remote Atlantic warming (Figure S1f), in contrast to the HIST simulation (Figure S1d). The ATL run captures qualitatively the observed SST cooling and positive SLP trends in the extratropical North and South Pacific (see Figure S1).

In relation to the observed principal components, there are some notable differences in the model simulated time series in GLOB, eqPAC, and ATL runs. Whereas the simulated SVD principal components for observations

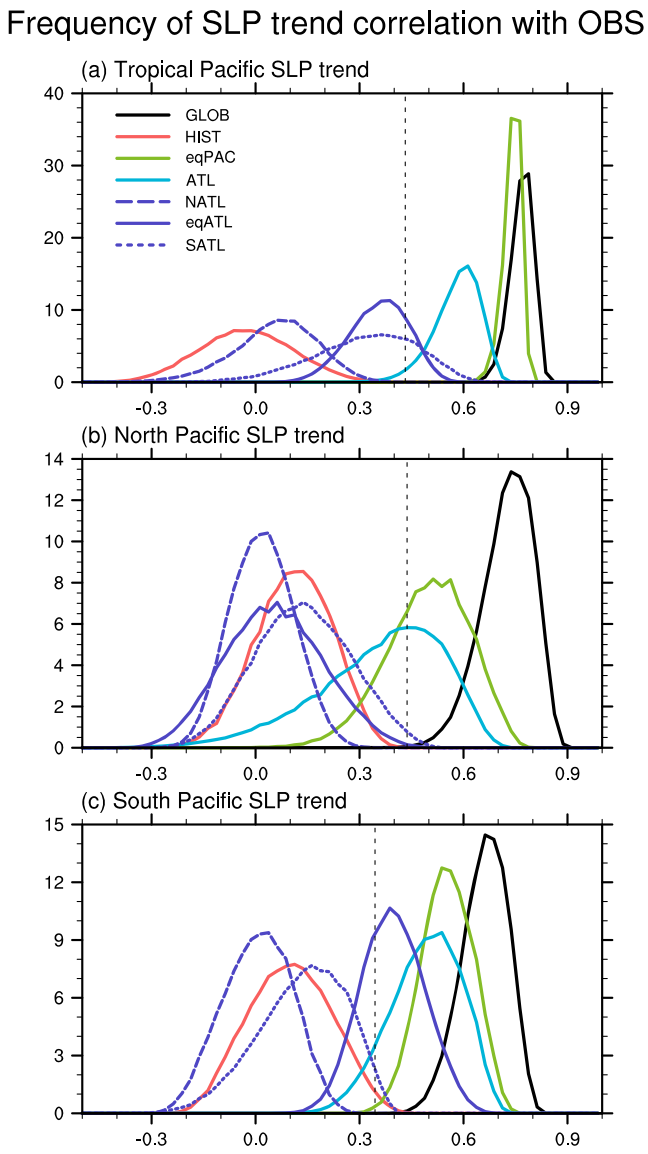

Figure 3. Frequency distributions in correlation coefficients of 9 year running trends (a) for the tropical (15°S–15°N, 180°–150°W), (b) North (20°N–40°N, 180°–120°W), and (c) South Pacific SLP anomalies (40°S–20°S, 180°–120°W) between the observation (HadSLP2r) and the model experiments of GLOB (black), HIST (red), eqPAC (green), ATL (light blue), NATL (purple dashed), eqATL (purple solid), and SATL runs (purple dotted). Frequency distributions are obtained from the bootstrap method with 100,000 random samplings from 10 ensemble members in each experiment (see main text for details). Vertical dotted lines correspond to the statistical significance at 90% level on the basis of one-side Student's *t* test with the effective sample sizes estimated from 1 year lag autocorrelation coefficient.

and the eqPAC and ATL runs show coherent variations with those in GLOB ($R = 0.80$ and 0.55, respectively), they have only weak correlation with each other ($R = 0.26$). We also find that the time series for ATL shows the maximum correlation with those from the GLOB and eqPAC SVD analysis at 1 year lead ($R = 0.67$ and 0.38, respectively). This lead relationship further supports the notion that the Atlantic SST anomalies contribute to the generation of Pacific decadal SLP trends.

To further illustrate the effect of Atlantic SST changes on decadal SLP variability in the Pacific, we calculated the frequency distributions of the correlation coefficients of 9 year SLP running trend variability between observations and GLOB, ATL, eqPAC, and HIST runs using a bootstrap approach by exploiting the fact that we have 10 ensemble members for each simulation (Figure 3). For the index regions in consideration, we generate 100,000 new ensemble mean time series of 9 year SLP running trends by conducting the following

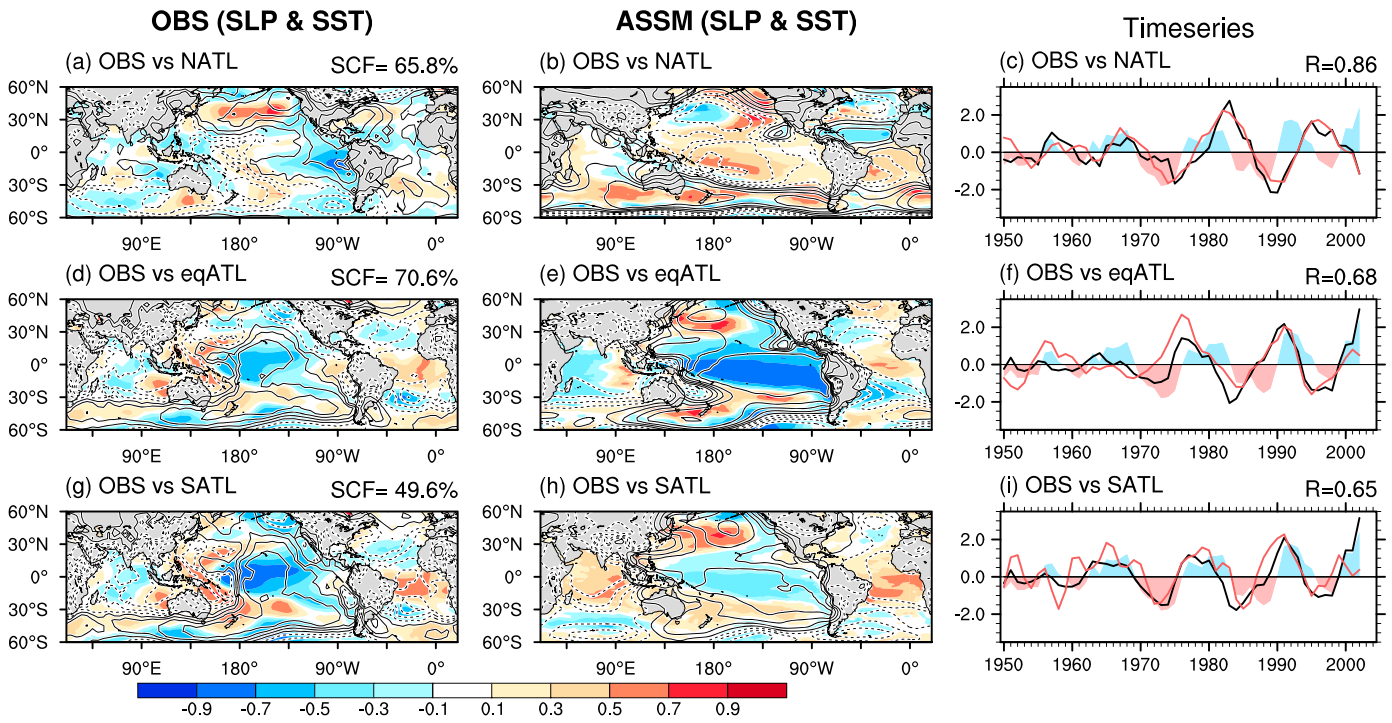

Figure 4. Same as Figure 2 but for (a–c) NATL, (d–f) eqATL, and (g–i) SATL runs.

procedure: a random 10-member ensemble is picked from the existing 9 year trends of the 10-member assimilation runs, allowing also for duplication (e.g., we may pick a combination such as [1, 4, 3, 9, 8, 9, 1, 1, 2, 3], where the number stands for the number in the initial ensemble member of assimilation run). For the randomly picked 10-member ensemble, we calculate the ensemble mean and correlate it with the observational estimate for the 9 year SLP running trend. This process allows us to calculate a probability distributions of correlation coefficients between the ensemble and the observations for each experiment (Figure 3). The significant correlation of the SLP trend variability in the tropical Pacific between observations and the eqPAC run as well as with the GLOB run (green and black lines in Figure 3a) is indicative of the strong atmosphere/ocean coupling in the tropical Pacific region. Furthermore, the observed tropical Pacific SLP trend is also reproduced in the ATL run (light blue in Figure 3a). In addition to the high SLP correlations in the tropical Pacific region between ATL and observations, we can also identify the significant correlations for the North and South Pacific regions. There, the effect of Atlantic forcing is comparable to that simulated in the eqPAC run (Figures 3b and 3c). The effects of Atlantic SST forcing on extratropical SLP trends can also be seen in Figures 2j and 2k. Our results clearly show that the Atlantic ocean remotely influences regional atmospheric changes in the tropical Pacific, along the west coast of North America, and the east coast of Australia.

To identify which region in the Atlantic is mainly responsible for the atmospheric teleconnections to the Pacific, we compare a series of partial assimilation experiments using only North, equatorial, and South Atlantic ocean data. The leading Pacific SLP SVD mode and its associated global correlation patterns between the equatorial Atlantic partial assimilation experiment (eqATL) and the observations show joint SST cooling in the equatorial Pacific and the surrounding subtropical/extratropical Pacific warming as well as good qualitative agreement with the observed Pacific SLP trend pattern (Figures 4d and 4e). Similar Pacific responses are also found in SATL run (Figures 4g and 4h), although the squared covariance fraction explained by the first SVD mode is smaller in SATL than eqATL runs (49.6% and 70.6% , respectively). In contrast, these SST and SLP trend patterns cannot be identified in the NATL run (Figures 4a and 4b). We find only a weak correlation of the first principal component time series in the GLOB run and the NATL experiment (Figure 4c) of $R = 0.21$, compared to the much higher values in the eqATL and SATL partial assimilation experiments ($R = 0.50$ and 0.77, respectively). The comparison of these partial assimilation experiments implies that the equatorial and South

Atlantic SST anomalies play a discernible role in generating tropical Pacific decadal-scale climate variability and the corresponding trends of the IPO since the 1990s. In fact, we can find positive correlations between observations and the ensemble realizations of the eqATL run for the equatorial and South Pacific SLP trend variability, which corresponds to about statistical significance at 90% level (purple solid in Figures 3a and 3c) as well as the contribution from SATL to the tropical Pacific SLP trend (purple dotted in Figure 3a).

According to the concept of transbasin variability proposed in previous studies [*McGregor et al.*, 2014; *Chikamoto et al.*, 2015], warmer surface conditions in the equatorial Atlantic relative to the Pacific create a transbasin SLP gradient and a corresponding reorganization of the global Walker Circulation with ascending air over the Atlantic and descending air over the eastern tropical Pacific. During the 1992–2000 period, for example, resulting central Pacific trade wind intensification cooled the central to eastern tropical Pacific, which influenced SLP trends in the extratropical Pacific via atmospheric teleconnections (Figure S1f). The response of the global Walker Circulation is also illustrated by the trends of the upper level atmospheric wind divergence associated with the first SLP SVD modes (Figure S4) between observations and model simulations. We find an upper level atmospheric wind divergence (convergence) over the western (eastern) tropical Pacific in GLOB, eqPAC, ATL, eqATL, and SATL runs (Figure S4) although centers of these divergence/convergence trends are slightly shifted westward in the ATL, eqATL, and SATL runs compared to the GLOB run. This upper level divergence pattern can strengthen the Pacific Walker Circulation and then cause the La Niña-like atmosphere-ocean response in the tropical Pacific. These features are missing in the HIST and NATL runs (Figures S4c and S4e).

4. Discussion and Conclusion

We have examined the relative impacts of Atlantic SST anomalies on Pacific climate decadal trends. The analysis was based on partial assimilation experiments, in which three-dimensional temperature and salinity ocean data were assimilated either globally or in the equatorial Pacific, the entire Atlantic, the equatorial, South, and North Atlantic regions. In contrast to SST-forced atmospheric general circulation model experiments, the partially assimilated approach allows for remote atmosphere-ocean interactions. Moreover, our method minimizes an artificial model drift by removing the climatological model biases.

Consistent with previous studies, our partial equatorial Pacific Ocean assimilation experiment simulates a slowdown of global mean SAT trends from 2000 to 2010 (Figure 1a). In addition, Atlantic SST anomalies are required to capture the trends in global mean SAT. According to our partial assimilation experiments, equatorial Atlantic SST anomalies contribute to the eastern Pacific cooling and to the SLP trends in the tropical, North, and South Pacific. South Atlantic SST forcing also excites atmospheric anomalies over the tropical Pacific (Figures 3 and S4). Extratropical North Atlantic SST changes associated, e.g., with Atlantic Multidecadal Variability [*Enfield et al.*, 2001; *Knight et al.*, 2006; *Ting et al.*, 2009] and historical radiative forcings have been found to play only a minor role in setting up transbasin variability and the recent observed decadal trends in global climate.

The origin of the observed equatorial Atlantic SST trends still remains elusive. To complicate matters further in our modeling experiments, there is a clear indication (Figures 2g–2i, SVD between observations and eqPAC) that a negative IPO also can induce Atlantic warming. The exact lead/lag relationships and the respective seasonality between equatorial Pacific and Atlantic SST forcing need to be further explored to elucidate the concerted activity of decadal tropical climate variability.

Our study, among with others [*Timmermann et al.*, 1998, 2007; *Okumura et al.*, 2009; *Kucharski et al.*, 2011; *Chikamoto et al.*, 2012; *McGregor et al.*, 2014; *Chikamoto et al.*, 2015; *Kucharski et al.*, 2015; *Li et al.*, 2015b], highlights the importance of understanding decadal climate variability in a multibasin context. The importance of transbasin teleconnections through shifts of the global Walker Circulation has to be considered in explaining the unprecedented negative IPO trend, as well as the slowdown or acceleration of global mean SAT. In addition to the Atlantic and the Pacific, SST trends over the tropical Indian Ocean and Maritime Continent may impact transbasin interactions as suggested previously [*Luo et al.*, 2012; *Han et al.*, 2014; T. Mochizuki et al., Inter-basin influence of the Indian Ocean on the Pacific decadal climate change, submitted by *Geophysical Research Letters*, 2016]. We hope that more coordinated future multimodel experiments will shed further light onto the tropical transbasin linkages and their role in past and future climate.

Acknowledgments
This study was supported by the Japanese Ministry of Education, Culture, Sports, Science and Technology, through the Program for Risk Information on Climate Change. The simulations were performed with the Earth Simulator at the Japan Agency for Marine-Earth Science and Technology. HadCRUT4, HadSLP2r/ERSST, and ERA-Interim data sets are provided by Met Office Hadley Centre, the NOAA/OAR/ESRL PSD, Boulder, Colorado, USA, from their Web site at http://www.esrl.noaa.gov/psd/, and ECMWF, respectively. The data in assimilation experiments are available from the authors upon request for research purpose. The manuscript benefited from the constructive comments of two anonymous reviewers. A.T. and Y.C. were supported by NSF (1049219).

References

Allan, R., and T. Ansell (2006), A new globally complete monthly historical gridded mean sea level pressure dataset (HadSLP2): 1850–2004, *J. Clim.*, *19*(22), 5816–5842.

Bloom, S. C., L. Takacs, A. M. da Silva, and D. Ledvina (1996), Data assimilation using incremental analysis updates, *Mon. Weather Rev.*, *124*, 1256–1271.

Chikamoto, Y., M. Kimoto, M. Watanabe, M. Ishii, and T. Mochizuki (2012), Relationship between the Pacific and Atlantic stepwise climate change during the 1990s, *Geophys. Res. Lett.*, *39*, L21710, doi:10.1029/2012GL053901.

Chikamoto, Y., A. Timmermann, J.-J. Luo, T. Mochizuki, M. Kimoto, M. Watanabe, M. Ishii, S.-P. Xie, and F.-F. Jin (2015), Skillful multi-year predictions of tropical trans-basin climate variability, *Nat. Commun.*, *6*, 6869.

Dee, D., et al. (2011), The ERA-Interim reanalysis: Configuration and performance of the data assimilation system, *Q. J. R. Meteorol. Soc.*, *137*(656), 553–597.

Delworth, T. L., F. Zeng, A. Rosati, G. A. Vecchi, and A. T. Wittenberg (2015), A link between the hiatus in global warming and North American drought, *J. Clim.*, *28*(9), 3834–3845.

Easterling, D. R., and M. F. Wehner (2009), Is the climate warming or cooling?, *Geophys. Res. Lett.*, *36*, L08706, doi:10.1029/2009GL037810.

Enfield, D. B., A. M. Mestas-Nunez, and P. J. Trimble (2001), The Atlantic multidecadal oscillation and its relationship to rainfall and river flows in the continental US, *Geophys. Res. Lett*, *28*, 2077–2080.

England, M. H., S. McGregor, P. Spence, G. A. Meehl, A. Timmermann, W. Cai, A. S. Gupta, M. J. McPhaden, A. Purich, and A. Santoso (2014), Recent intensification of wind-driven circulation in the Pacific and the ongoing warming hiatus, *Nat. Clim. Change*, *4*(3), 222–227.

Han, W., et al. (2014), Intensification of decadal and multi-decadal sea level variability in the western tropical Pacific during recent decades, *Clim. Dyn.*, *43*(5-6), 1357–1379.

Huang, B., J. Kinter, and P. Schopf (2002), Ocean data assimilation using intermittent analyses and continuous model error correction, *Adv. Atmos. Sci.*, *19*(6), 965–992.

Huang, B., V. F. Banzon, E. Freeman, J. Lawrimore, W. Liu, T. C. Peterson, T. M. Smith, P. W. Thorne, S. D. Woodruff, and H.-M. Zhang (2015), Extended reconstructed sea surface temperature version 4 (ERSST. v4). Part I: Upgrades and intercomparisons, *J. Clim.*, *28*(3), 911–930.

Ishii, M., and M. Kimoto (2009), Reevaluation of historical ocean heat content variations with time-varying XBT and MBT depth bias corrections, *J. Oceanogr.*, *65*(3), 287–299.

Knight, J., C. Folland, and A. Scaife (2006), Climate impacts of the Atlantic multidecadal oscillation, *Geophys. Res. Lett.*, *33*, L17706, doi:10.1029/2006GL026242.

Kosaka, Y., and S.-P. Xie (2013), Recent global-warming hiatus tied to equatorial Pacific surface cooling, *Nature*, *501*(7467), 403–407.

Kucharski, F., I. Kang, R. Farneti, and L. Feudale (2011), Tropical Pacific response to 20th century Atlantic warming, *Geophys. Res. Lett.*, *38*, L03702, doi:10.1029/2010GL046248.

Kucharski, F., F. Ikram, F. Molteni, R. Farneti, I.-S. Kang, H.-H. No, M. P. King, G. Giuliani, and K. Mogensen (2015), Atlantic forcing of Pacific decadal variability, *Clim. Dyn.*, *46*, 2337–2351.

Li, C., B. Stevens, and J. Marotzke (2015a), Eurasian winter cooling in the warming hiatus of 1998–2012, *Geophys. Res. Lett.*, *42*, 8131–8139, doi:10.1002/2015GL065327.

Li, X., S.-P. Xie, S. T. Gille, and C. Yoo (2015b), Atlantic-induced pan-tropical climate change over the past three decades, *Nat. Clim. Change*, *6*, 275–279, doi:10.1038/nclimate2840.

Luo, J.-J., W. Sasaki, and Y. Masumoto (2012), Indian Ocean warming modulates Pacific climate change, *Proc. Natl. Acad. Sci.*, *109*(46), 18,701–18,706.

McGregor, S., A. Timmermann, M. F. Stuecker, M. H. England, M. Merrifield, F.-F. Jin, and Y. Chikamoto (2014), Recent Walker circulation strengthening and Pacific cooling amplified by Atlantic warming, *Nat. Clim. Change*, *4*(10), 888–892.

Meehl, G. A., and H. Teng (2014), Regional precipitation simulations for the mid-1970s shift and early-2000s hiatus, *Geophys. Res. Lett.*, *41*, 7658–7665, doi:10.1002/2014GL061778.

Meehl, G. A., J. M. Arblaster, J. T. Fasullo, A. Hu, and K. E. Trenberth (2011), Model-based evidence of deep-ocean heat uptake during surface-temperature hiatus periods, *Nat. Clim. Change*, *1*(7), 360–364.

Merrifield, M. A., and M. E. Maltrud (2011), Regional sea level trends due to a Pacific trade wind intensification, *Geophys. Res. Lett.*, *38*, L21605, doi:10.1029/2011GL049576.

Mochizuki, T., et al. (2010), Pacific decadal oscillation hindcasts relevant to near-term climate prediction, *Proc. Natl. Acad. Sci. USA*, *107*, 1833–1837, doi:10.1073/pnas.0906531107.

Morice, C. P., J. J. Kennedy, N. A. Rayner, and P. D. Jones (2012), Quantifying uncertainties in global and regional temperature change using an ensemble of observational estimates: The HadCRUT4 data set, *J. Geophys. Res.*, *117*, D08101, doi:10.1029/2011JD017187.

Nakicenovic, N., et al. (2000), *Emissions Scenarios, A Special Report of Working Group III of the Intergovernmental Panel on Climate Change*, Cambridge Univ. Press, New York.

Nieves, V., J. K. Willis, and W. C. Patzert (2015), Recent hiatus caused by decadal shift in Indo-Pacific heating, *Science*, *349*(6247), 532–535.

Nozawa, T., T. Nagashima, T. Ogura, T. Yokohata, N. Okada, and H. Shiogama (2007), Climate change simulations with a coupled ocean-atmosphere GCM called the model for interdisciplinary research on climate: MIROC, *CGER Supercomput. Monogr. Rep. 12*, Center for Global Environmental Research, National Institute for Environmental Studies, Tsukuba, Jpn.

Okumura, Y. M., C. Deser, A. Hu, A. Timmermann, and S.-P. Xie (2009), North Pacific climate response to freshwater forcing in the subarctic North Atlantic: Oceanic and atmospheric pathways, *J. Clim.*, *22*(6), 1424–1445.

Robson, J., R. Sutton, K. Lohmann, D. Smith, and M. D. Palmer (2012), Causes of the rapid warming of the North Atlantic Ocean in the mid 1990s, *J. Clim.*, *25*, 4116–4134, doi:10.1175/JCLI-D-11-00443.1.

Timmermann, A., M. Latif, R. Voss, and A. Grötzner (1998), Northern hemispheric interdecadal variability: A coupled air-sea mode, *J. Clim.*, *11*(8), 1906–1931.

Timmermann, A., et al. (2007), The influence of a weakening of the Atlantic meridional overturning circulation on ENSO, *J. Clim.*, *20*(19), 4899–4919.

Timmermann, A., S. McGregor, and F.-F. Jin (2010), Wind effects on past and future regional sea level trends in the Southern Indo-Pacific, *J. Clim.*, *23*(16), 4429–4437, doi:10.1175/2010JCLI3519.1.

Ting, M., Y. Kushnir, R. Seager, and C. Li (2009), Forced and internal twentieth-century SST trends in the North Atlantic, *J. Clim.*, *22*(6), 1469–1481.

Trenberth, K. E., and J. T. Fasullo (2013), An apparent hiatus in global warming?, *Earth's Future*, *1*(1), 19–32.

Watanabe, M., Y. Kamae, M. Yoshimori, A. Oka, M. Sato, M. Ishii, T. Mochizuki, and M. Kimoto (2013), Strengthening of ocean heat uptake efficiency associated with the recent climate hiatus, *Geophys. Res. Lett.*, *40*, 3175–3179, doi:10.1002/grl.50541.

Yeager, S., A. Karspeck, G. Danabasoglu, J. Tribbia, and H. Teng (2012), A decadal prediction case study: Late twentieth-century North Atlantic ocean heat content, *J. Clim.*, *25*(15), 5173–5189.

Zhang, R., and T. L. Delworth (2007), Impact of the Atlantic multidecadal oscillation on North Pacific climate variability, *Geophys. Res. Lett.*, *34*, L23708, doi:10.1029/2007GL031601.

Supporting Information for

"Potential tropical Atlantic impacts on Pacific decadal climate trends"

Y. Chikamoto[1], T. Mochizuki[2], A. Timmermann[1], M. Kimoto[3], and M. Watanabe[3]

[1]International Pacific Research Center, University of Hawaii at Manoa, Honolulu, Hawaii, USA

[2]Japan Agency for Marine-Earth Science and Technology, Yokohama, Japan

[3]Atmosphere and Ocean Research Institute, University of Tokyo, Kashiwa, Japan

Contents

Figures

Corresponding author: Y. Chikamoto, chika44@hawaii.edu

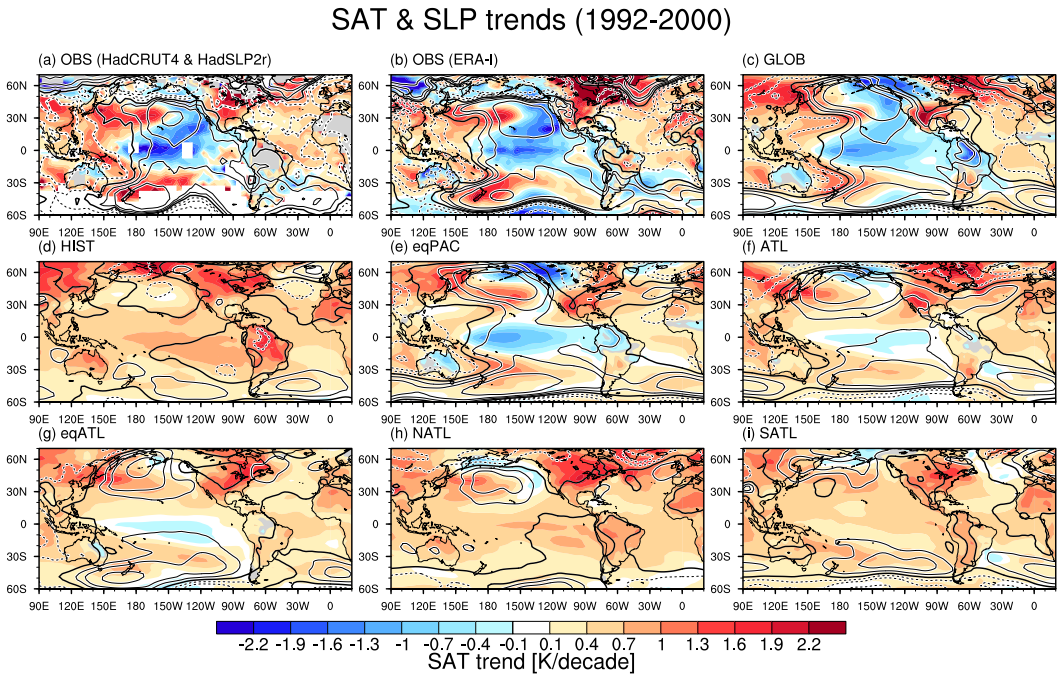

Figure S1. Nine-year trend maps of SAT (shading) and SLP (contour) anomalies during 1992–2000 in (a) HadCRUT4 and HadSLP2r, (b) ERA-I, (c) GLOB, (d) HIST, (e) eqPAC, (f) ATL, (g) eqATL, (h) NATL, and (i) SATL runs. Contour intervals are $\pm 0.5, \pm 1, \pm 2, \pm 5, \pm 10, \pm 20$ hPa/decade.

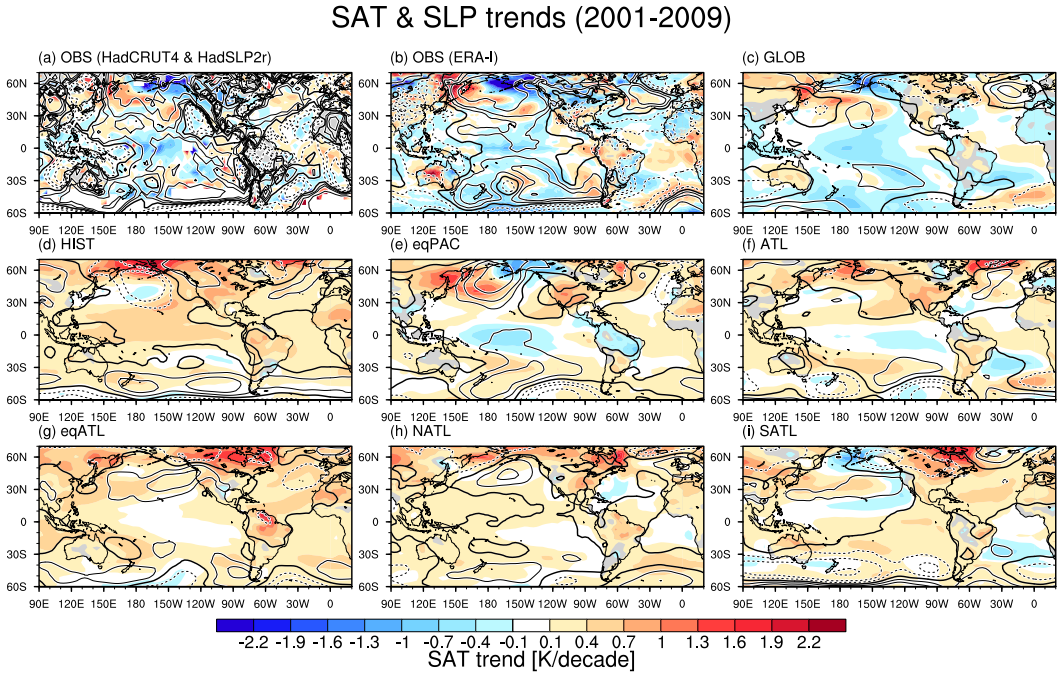

Figure S2. Same as Fig. S1 but for 2001–2009.

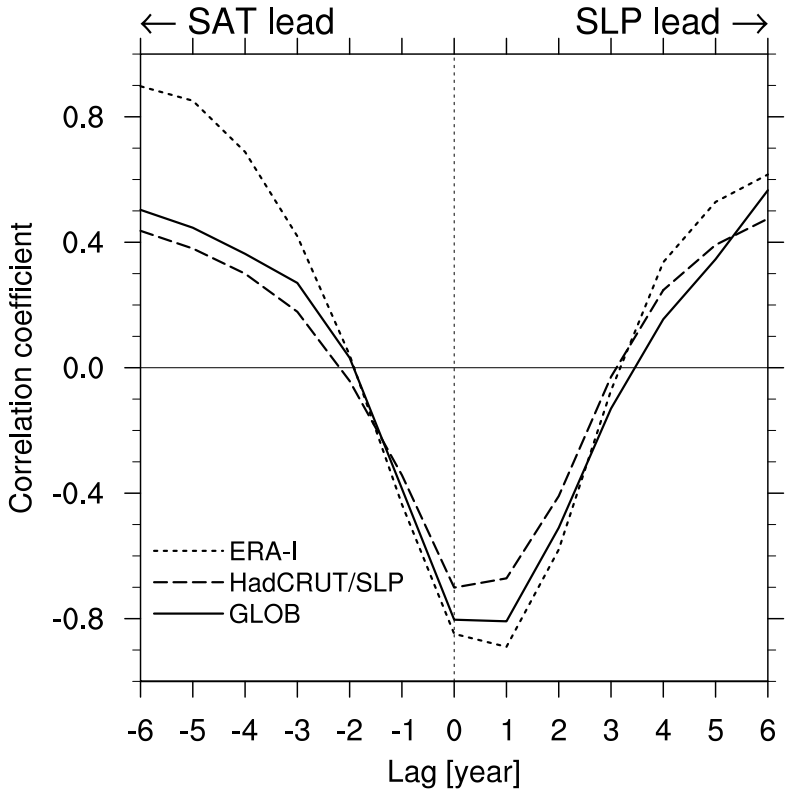

Figure S3. Lag correlation coefficient between 9-year running trends of the eastern tropical Pacific SAT and the central tropical Pacific SLP. Positive lag indicates that SLP leads. Solid, dashed and dotted lines are GLOB run, HadCRUT4/HadSLP2r, and ERA-I data, respectively.

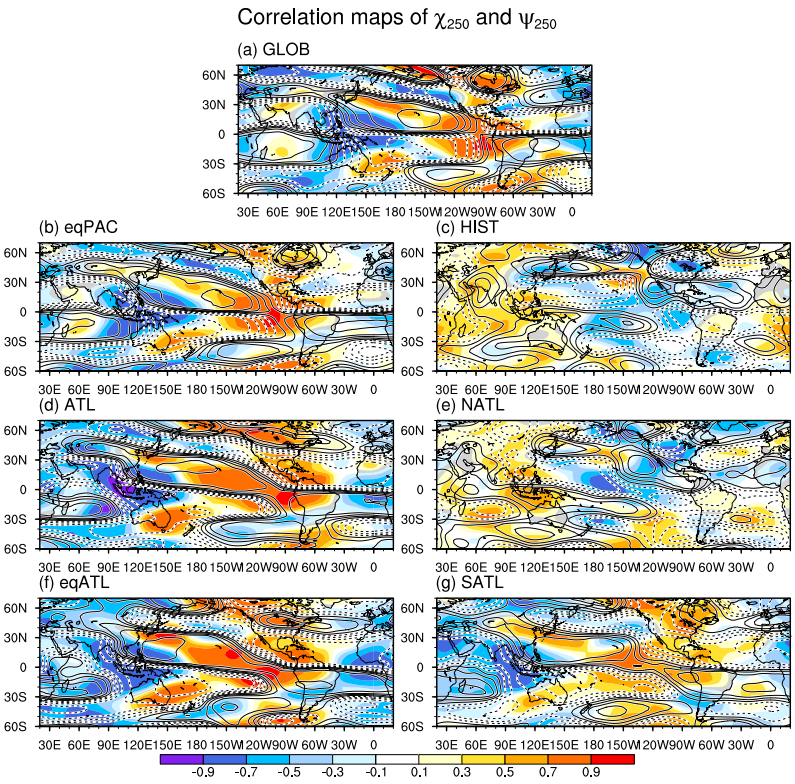

Figure S4. Correlation maps of 9-year running trends in velocity potential (shading; the positive anomalies represent the wind convergence) and stream function (contour) at 250 hPa with the model simulated time series of the first SLP SVD modes between observations and the experiments of (a) GLOB, (b) eqPAC, (c) HIST, (d) ATL, (e) NATL, (f) eqATL, and (g) SATL runs (red lines in Figs. 2c, 2i, 2f, 2l, 4c, 4f, and 4i). Negative contours are dashed and zero contours are omitted. Contour intervals are ± 0.1, ± 0.3, ± 0.5, ± 0.7, and ± 0.9.